RSC Advances

ROYAL SOCIETY OF CHEMISTRY

www.rsc.org/advances

Journal Name

RSCPublishing

ARTICLE

The Role of Silver Nanoparticles Functionalized on TiO_2 for Photocatalytic Disinfection of Harmful Algae

Cite this: DOI: 10.1039/x0xx00000x

Soo-Wohn Lee,[a] S. Obregón,[b,c] and V. Rodríguez-González[d]

Received ooth January 2012,
Accepted ooth January 2012

DOI: 10.1039/x0xx00000x

www.rsc.org/

Silver loaded TiO_2 samples were prepared by photodeposition of different amounts of Ag^+ ions over commercial titanium dioxide (Evonik TiO_2 P25) in aqueous media without the presence of sacrificial agents. The obtained photocatalysts were characterized by several techniques such as X-ray powder diffraction (XRD), UV-Vis diffuse reflectance spectroscopy (DRS), transmission electron microscopy (TEM) and X-ray photoelectron spectroscopy (XPS) in order to correlate the effect of the silver amount on the photocatalytic properties of the final nanocomposite. The effect of the silver nanoparticles on the photocatalytic behaviour of TiO_2 was evaluated by means of the photodegradation of methyl orange dye and the inactivation of noxious algae *Tetraselmis suecica* and *Amphidium carterae* under continuous exposure of low power irradiation UV-light. The sample with 1.5% wt. of silver nanoparticles showed the highest photocatalytic elimination of the azo dye and both algae types. According to the results, the cells were deformed during the photocatalytic process by the attack of highly reactive species such as hydroxyl radicals, H_2O_2 and superoxide ions generated on the TiO_2 surface. The algae cells were not regenerate by themselves after photocatalytic process due the high degree of fragmentation that suffered during the light irradiation.

1. Introduction

The algal population level of a water body is an indicator of the water pollution status.[1] For example, the excessive growth of the microalgae *Amphidium carterae* indicates oil pollution of water bodies.[2] The increase in the amount of organic matter that is added to water bodies results in an increase in the nutrient supply for the growth of microorganisms, a phenomenon known as eutrophication.[2] When extremely high levels of nutrients are present in the water, the microorganism blooms can lead to cell clumps which grow, die and accumulate leaving floating mats of decomposing organic matter. Sometimes, such cells release toxins which may be highly harmful to aquatic life, causing death, which in return causes serious problems to human health.[3-5] An emerging option for removing harmful algae bloom is the photocatalysis. The sterilization of microbial cells in water by this green photochemical process was first reported by Matsunaga and co-workers.[6] They used a TiO_2/Pt powder catalyst which upon illumination with near-UV light kills the *Lactobacillus acidophilus*, *Saccharomyces cerevisiae*, and *Escherichia coli* bacteria. Since this report, many other studies have been reported for the successful removal of pathogenic microorganisms with TiO_2 powders as well as TiO_2 thin films.[7,8] For example, Linkous and co-workers studied the photocatalytic effect of TiO_2 and WO_3 coatings in the presence and absence of Pt and Ir as co-catalysts for the elimination of the filamentous *Oedogonium* algae.[9] These authors found that by using a combination of black light and fluorescent lamps, a cement surface coated with TiO_2 was highly effective in the inhibition of the growth of *Oedogonium* algae in comparison with the uncoated cement.

Recently, we have demonstrated the effective use of several photocatalysts for the complete removal of noxious microalgae such as *Amphidium carterae*, also known as "red tide" due to the characteristic colour of their floating dead cells.[10-12] Following this research line, the present work reports the photocatalytic effect on the elimination of the harmful microalgae *A. carterae* and *T. suecica* by using different amounts of Ag nanoparticles photodeposited on commercial titanium dioxide (Evonik TiO_2 P25) under near UV-irradiation.

2. Experimental

2.1 Preparation of silver-TiO_2 powder samples

Silver-TiO_2 loaded samples were prepared by the photo-impregnation method, which has been described previously.[10] For this purpose, Evonik TiO_2 P25 was used as the titanium dioxide source. To prepare 1 wt. % of Ag nanoparticles loaded on the TiO_2 surface, 0.472 g of silver nitrate (Samchun, 99.8%) were added to 1L of distilled water and placed in a ultrasound bath for 5 min in order to ensure complete disaggregation. Afterwards, 29.7 g of Evonik TiO_2 P25 were added to the silver aqueous solution and the slurry was stirred vigorously for 1h in order to achieve the adsorption-desorption equilibrium of Ag^+ ions on the TiO_2 surface. Then, the mixture was exposed to UV

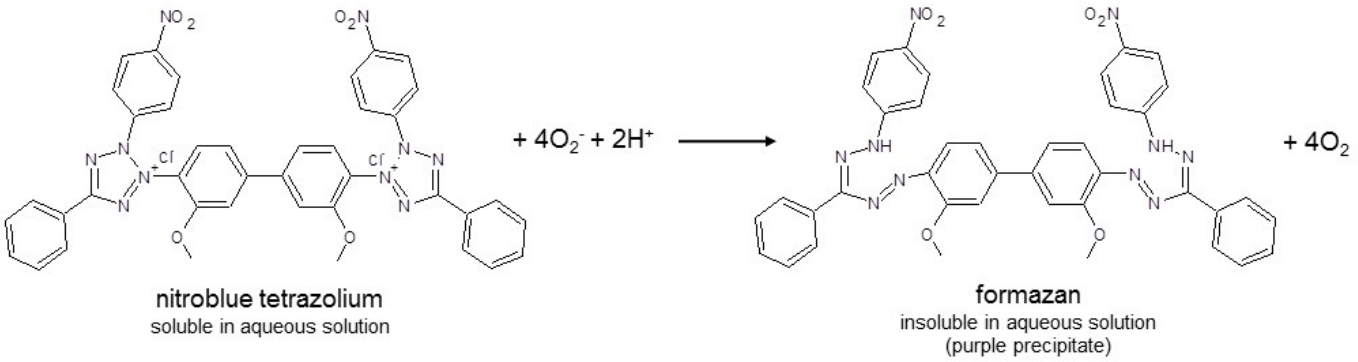

Scheme 1. Reaction of nitroblue tetrazolium with the superoxide ion.

light for 2h using two 20W V lamps (Black light lamp-BL, Sankyo Denky, Japan). After, the slurry was dried in a vacuum rotary evaporator at 80 °C for 4h. The resulting powder was heated at 100 °C for 12h and then stored under dark conditions. Identical procedures were performed in order to prepare the samples with other amounts of silver nanoparticles.

2.2. Characterization of Materials

The structural characterization was carried out by X-ray powder diffraction using a Bruker D8 Advanced diffractometer with CuKα radiation. X-ray diffraction data of the samples were recorded between 10 and 70° (2θ). X-ray photoelectron spectroscopy measurements were obtained with an ESCA-3200 Shimadzu electron spectrometer equipped with a hemispherical analyzing system. The spectrometer was operated with monochromatic MgKα X-rays (1253.6 eV) at 30 mA and 8 kV. The binding energies were referenced to the C 1s peak at 284.6 eV of the adventitious surface carbon. Diffuse reflectance spectra were measured with a Perkin-Elmer Lambda 35 UV-Vis spectrophotometer equipped with an integrating sphere. The used reference sample was a $BaSO_4$ coated standard pattern. The size of the Ag nanoparticles was estimated by transmission electron microscopy using a JEM2200FS JEOL microscope with spherical aberration correction in a STEM mode and working with an accelerating voltage of 200 keV. To prepare the materials for the study, powdered samples were dispersed in ethanol and supported on carbon-coated copper grids.

2.3. Photocatalytic tests

The photocatalytic activity of the Ag-TiO_2 samples was firstly tested through the photodegradation of the methyl orange dye (Methyl Orange A.C.S, Aldrich) used as model reaction.[13] The light irradiation source consisted of a standard Pen-Ray UV lamp (UVP Products) with an intensity of 4400 $\mu W \cdot cm^{-2}$ at 254 nm. In a typical experiment, 250 mg of photocatalyst was added to a home-made reactor containing 250 mL of a methyl orange solution with an initial concentration of 35 $mg \cdot L^{-1}$. In order to reach the adsorption-desorption equilibrium, a dry air flow was bubbled to the reactant solution during 30 min under dark conditions and stirring. When the lamp was turn on, aliquots were taken at given irradiation times and after filtered through a nylon filter. The methyl orange concentration was followed through the evolution of the characteristic 465 nm band using the centrifuged aliquots. The blank test was run without catalyst and no methyl orange degradation was observed after 3h.

The photocatalytic production of the superoxide ion (O_2^-) was evaluated under the same conditions as the degradation of methyl orange dye. As shown in Scheme 1, the nitroblue tetrazolium (NBT) can be specifically reduced by the superoxide ion (O_2^-) in order to form the insoluble purple formazan.[14] The photocatalytic tests were made with an initial concentration of NBT 5×10^{-5} $mol \cdot L^{-1}$ and a 0.5 $g \cdot L^{-1}$ concentration of the photocatalyst. The production of the superoxide ion was quantitatively analyzed through the evolution of the absorption maximum at 259 nm of the nitroblue tetrazolium.

The photocatalytic disinfection tests were carried out in a batch reactor according to previous reports.[11] In a glass beaker, 100 mg of a powdered sample were added to 200 mL of a dispersion of either *T. suecica* with an initial concentration of $240\pm10x10^3$ $cells \cdot mL^{-1}$ (Natural Live Plankton Co., Ltd., 99.9%) or *A. carterae* $150\pm10x10^3$ $cells \cdot mL^{-1}$ (Natural Live Plankton Co., Ltd., 99.9%). Then, the suspension was exposed to UV irradiation using two 20W UV-A lamps (Black light lamp-BL, Sankyo Denky, Japan). The experiment was carried out at room temperature under continuous stirring conditions. At given time intervals, 100 µL of the suspension were collected and analyzed to determine the concentration of the living cells. The counting of the living cells was performed using a Neubauer chamber, which consists of a ruled glass slide containing a central square area with a thickness of 0.1 mm. This chamber was filled with the aliquot and sealed with a coverslip. Then, about 30-100 living cells were counted at least three times for each sample at 40X under a Motic-BA200 optical microscope. The microalgae living cells show random movement, while the dead algae are immobile and their morphologies changed to a deformed round shape. The pH of the dispersion was monitored during the photocatalytic tests, although significant changes in pH were not observed.

3. Results and Discussions

3.1 Preparation and characterization of the samples

From XRD results, it was found that the samples show an intense diffraction peak at 25.4° (2θ) which corresponds to the plane (101) of the TiO_2 anatase crystalline phase, see Figure 1. The small diffraction peaks can be assigned to other known planes of anatase (PDF 21-1272) and rutile phase (PDF 21-1276). These results are consistent with the expected crystalline composition of the Evonik TiO_2 P25, a composition leading to a synergistic photocatalytic effect according previous studies.[10] Diffraction peaks assignable to either Ag or AgO were not

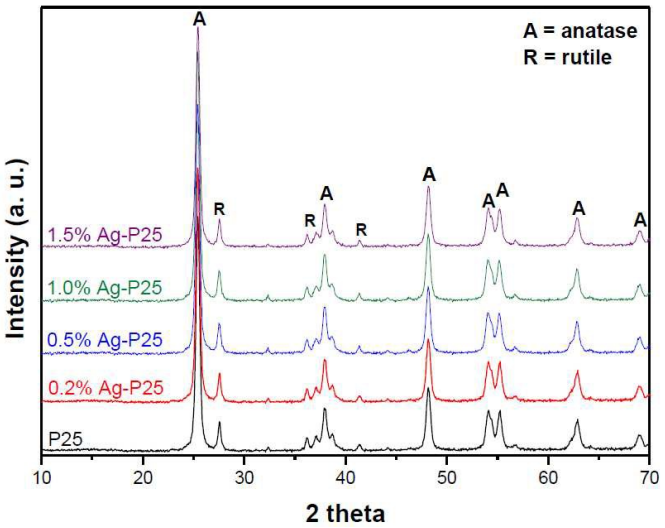

Figure 1. XRD patterns of the Ag loaded TiO_2 powders.

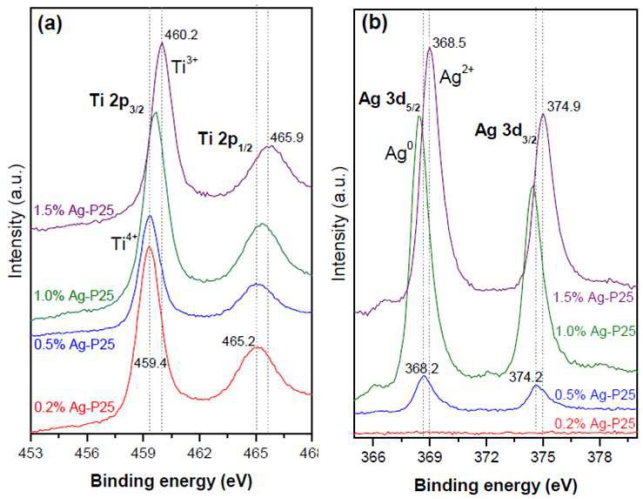

Figure 2. XPS spectra of (a) Ti 2p and (b) Ag 3d core levels for the Ag-TiO_2 photodeposited samples.

found due to the low concentration and/or high dispersion of the reduced metal photodeposited on the surface of the photocatalyst.

The energy band gap value for the sample without silver nanoparticles (P25) was estimated as 3.2 eV, which is the same as the one that has been reported previously.[15] A slight increase of the silver amount (0.2%) leads to decrease in the energy band gap and until a value of 2.98 eV is reached for the sample with 1.5% wt. of silver nanoparticles. Since photodeposition of silver nanoparticles on titanium dioxide do not change the positions of the valence and conduction band of TiO_2, the differences in the band gap of the samples are could be attributed to the surface plasmon absorption of spatially confined electrons in Ag nanoparticles.[16] The surface area values of the samples showed no changes from the value obtained for the Evonik TiO_2 P25 (~54 $m^2 \cdot g^{-1}$). These data confirm that the presence of silver nanoparticles do not affect the textural properties of the titanium oxide.

The XPS spectra of Evonik TiO_2 P25 loaded with different amounts of silver nanoparticles were analyzed. The Ti 2p spectra, shows Ti 2p XPS peaks at binding energies of 459.4 and 465.2eV, which are characteristic of the Ti^{4+} oxidation state in TiO_2, see Figure 2a.[16] On the other hand, Figure 2b shows the Ag 3d peaks where the binding energies for Ag agree fairly well with those reported for silver impregnated TiO_2 samples.[16] The Ag 3d peaks appear at a binding energy of 368.2 eV ($3d_{5/2}$) and the 3d doublet ($3d_{3/2}$) is located at approximately 374.2 eV. These binding energies indicate that a large amount of reduced silver particles exist on the TiO_2 support surface.[17] The peaks of the silver XPS spectra shows greater intensity with higher silver content. The 3d Ag peaks at 368.2 and 374.2 eV are characteristic of metallic Ag, while the shift of 3d Ag peaks at 374.9 and 368.9 eV could suggest the presence of silver particles with different sizes, which are normally assigned to the Ag_2O state.[17]

Figure 3(a-b) shows the TEM images of the samples with 1.0 and 1.5% wt. of silver nanoparticles. Samples with lower amounts of Ag nanoparticles were also examined. However, the silver nanoparticles were not observed probably due to their small sizes and low concentration. The average diameters of the anatase and rutile particles were estimated to be 25 and 85 nm, respectively, which is consistent with the results reported by Ohno and co-workers.[18] The toxicity of the silver nanoparticles depends on their size, where smaller sizes (≤ 10 nm) exhibit higher anti-microbial activity due to easier cell penetration.[19]

Particle size distribution of Ag nanoparticles was done from TEM micrographs by counting at least 300 particles from each sample, Figure 4(c-d). The results show silver nanoparticles with a very narrow size distribution and a predominant size of 4-5 nm for the sample with 1.0% wt. On the other hand, when the silver amount is 1.5%, a heterogeneous distribution is found in the 2-13 nm range with a typical size of 7-8 nm. Sclafani and Hermann proposed a mechanism that describes the deposition and growth of silver particles on the TiO_2 surface.[20] When titanium dioxide is irradiated with UV light, the formation of electron-hole pairs occurs by transferring electrons to the conduction band from the valence band as shown by Eq. 1:

$$TiO_2 + h\upsilon \rightarrow TiO_2\,(e^-, h^+) \qquad \text{Eq. 1}$$

Then, silver ions are initially adsorbed on the surface of TiO_2 particles and the photogenerated electrons reduce the Ag^+ ions to silver metal atoms:

$$TiO_2\,(e^-, h^+) + Ag^+_{adsorbed} \rightarrow TiO_2\,(h^+) + Ag^0 \qquad \text{Eq. 2}$$

It is possible that an increase in the silver amount causes the formation of larger particles during the growth stage:

$$mAg^0 \rightarrow Ag_m \qquad \text{Eq. 3}$$

3.2 Photocatalytic tests

The photocatalytic activity of the Ag-TiO_2 samples was tested by the degradation of methyl orange dye under UV irradiation.[21] The temporal evolution of the dye concentration during the photodegradation process is shown in Figure 4. As can be seen, the difference in the photodegradation of methyl orange dye between bare TiO_2 and 0.5% wt. Ag-TiO_2 is small, after 210 min of UV-light irradiation. Moreover, the photodegradation was increased using the 1% wt. Ag-TiO_2 sample. Also, the sample 1.5% wt. Ag-TiO_2 showed a similar degradation of the dye. The kinetic data can be adjusted

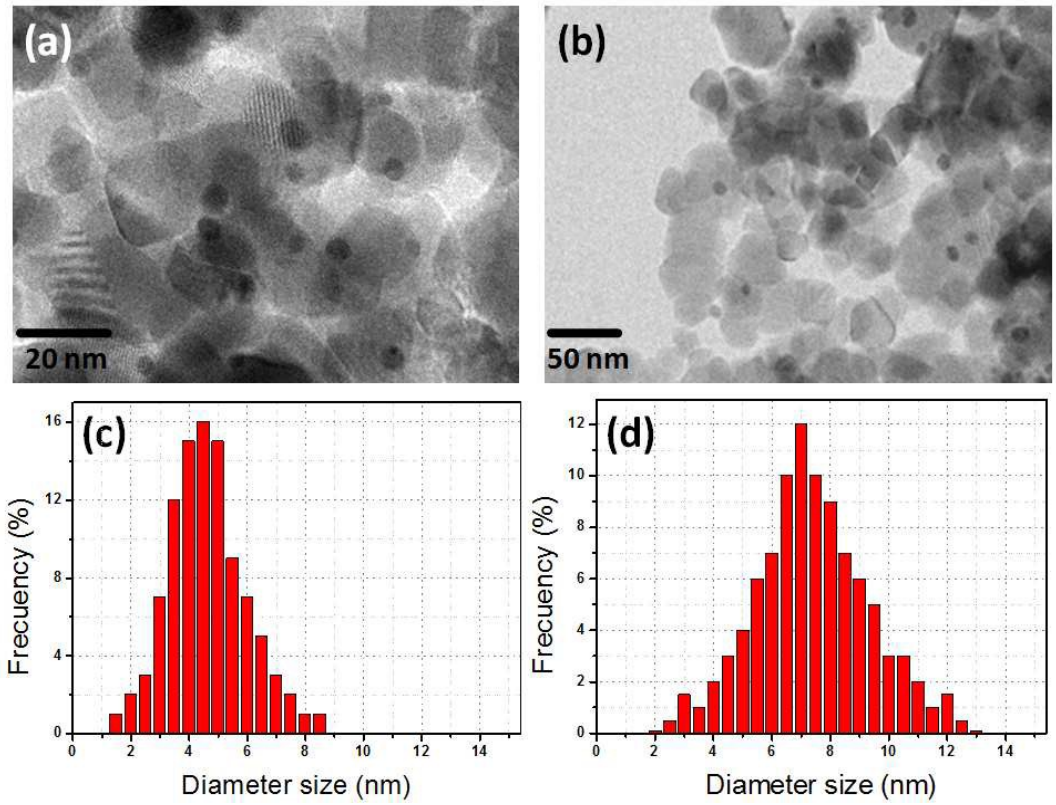

Figure 3. (a-b) Transmission Electron Microscopy and (c-d) particle size distribution of Evonik TiO_2 P25 samples impregnated with 1.0 and 1.5% of silver nanoparticles.

according with a first-order reaction equation following the Langmuir-Hinshelwood model. On the basis of this model, the half-life time for bleaching the methyl orange dye was 57.8 min for the 1.0% wt. Ag-TiO2 sample compared and 132 min for the bare TiO_2.

The photocatalytic production of the superoxide ion (O_2^-) was estimated by means the specific reduction reaction of the nitroblue tetrazolium molecule (NBT) by the superoxide ions. As shown in Figure 5, the bare TiO_2 led to the formation of a lower concentration of superoxide ions compared with the silver loaded samples. The trapping of the electron by oxygen molecule resulting in the formation of O_2^- is an effective pathway for promoting the separation of the photogenerated charge carriers. Therefore, these results show that the addition of silver nanoparticles on TiO_2 increase its photoactivity.

The photocatalytic performance of the photocatalysts also was evaluated for the elimination of noxious microalgae cells under UV-A irradiation. Figure 6 shows the rate constants for the photoelimination of *Tetraselmis suecica* cells in terms of the amount of Ag nanoparticles on the TiO_2 surface. According to the results, the increase in the silver amount promotes a considerable increase in the photocatalytic removal of the algae

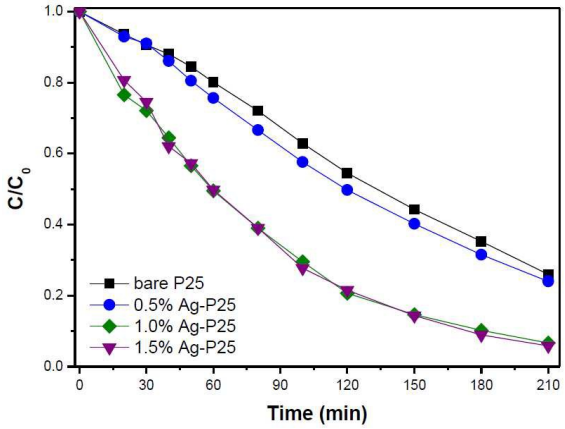

Figure 4. Photodegradation of methyl orange dye for the Ag loaded TiO_2 powders under UV-light irradiation.

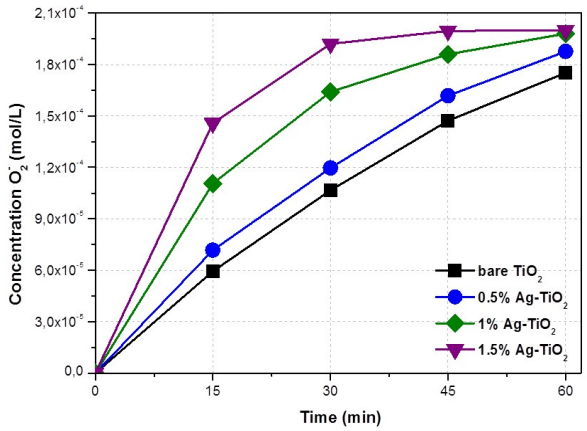

Figure 5. Photocatalytic production of superoxide ion (O_2^-) by Ag-TiO_2 samples under UV-light irradiation.

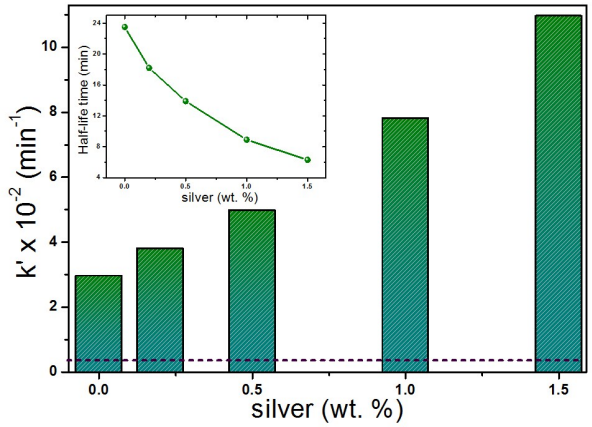

Figure 6. Rate constants and half-life time for *T. suecica* elimination as function of silver contents on TiO_2 samples.

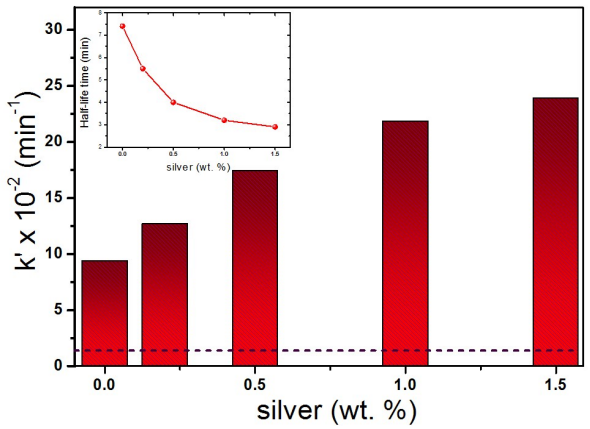

Figure 7. Rate constants and half-life time for *A. carterae* elimination as function of silver contents on TiO_2 samples.

cells. The dashed line with a value of $0.4x10^{-2}$ min^{-1} can be considered negligible and represents the rate constant of the system under UV light in absence of photocatalyst. In other words, the presence of UV light over *T. suecica* cells does not appear to cause damage at cellular level that could lead to the death of the algae. The top inset of Figure 6 shows the half-life time of the microalgae cells during the photocatalytic process. A semi-linear relationship is observed, which is consistent to the amount of silver nanoparticles on TiO_2. A half-life time of 23.5 min was obtained for the bare TiO_2 sample in the absence of silver nanoparticles. In the presence of 0.2% wt. of Ag nanoparticles, the half-life time was 18.2 min and continued decreasing as the Ag concentration was increased until a half-life time of 6.3 min was obtained. This half-life time corresponds to a value almost four times higher than that obtained with bare TiO_2. Normally, experiments in darkness are needed to confirm the photocatalytic effect by comparing the light versus darkness reactivity. In this particular case, the algae cells are photosynthetic and require light that their chloroplasts can absorb, increasing the concentration of living cells. However, it is clear that the presence of Ag impregnated TiO_2 photocatalysts under UV-light leads to a considerable decrease in the living algae cells. A comparison of micrographs showing the microalgae cells before and after the photocatalytic process indicates that photocatalysis damages clearly the structure of the cells (data not shown). The cells can be attacked by highly reactive species such as hydroxyl radicals, H_2O_2 and superoxide ions generated on the TiO_2 surface. After 8h of UV irradiation, the algae cells were deformed and annihilated thus preventing regeneration. After, nutritive water (Natural Live Plankton Co., Ltd.,) was added to the system and incubated at 25 ºC for 72 h. The suspension was analyzed to count the cell concentration, where living cells were not observed.

On the other hand, Figure 7 shows the rate constant for the photoelimination of the microalgae *Amphidium carterae*, where the dashed line represents the rate constant in absence of photocatalyst, which can be considered negligible. It is noteworthy to mention that the silver loaded samples showed a higher photocatalytic removal of living cells when the Ag nanoparticles are at higher concentration. However, the elimination of the cells did not represent a linear relationship with respect to the silver concentration in the samples. As it can be seen in the top inset of Figure 7, the half-life times are lower than those obtained in the elimination of the microalgae T. *suecica*. It is possible that *A. carterae* cells are less resistant to the hydroxyl radicals produced during the photocatalytic process and therefore these oxidative radicals cause damage more easily to the cell membranes, causing their death.

According to Ohno and co-workers, the rutile phase in TiO_2 P25 powder does not exist as an overlayer on the surface of anatase particles.[16] When the anatase and rutile particles are put in contact with aqueous media, the mixed phases must be the key to the high photocatalytic activity of the TiO_2 P25 powder. On the other hand, it is well known that the antimicrobial activity of the Ag nanoparticles is dependent on its size due to the ease with which they can be attached to the surface of the cells. This adhesion disturbs the cell membrane permeability and respiration functions of cells causing deformation and subsequent death.[17] Nevertheless, in our case this antimicrobial activity can be considered as a minimal effect, mainly because the Ag nanoparticles are not detached from the TiO_2 surface. This statement can be supported by a previous study by ICP analysis, where the lixiviation of silver nanoparticles from TiO_2 can be considered negligible under UV irradiation conditions.[8] Electron transfer from the TiO_2 conduction band to Ag nanoparticles is thermodynamically possible because the Fermi level of TiO_2 is higher than that of metallic silver. This phenomenon is expected to provide the formation of a Schottky barrier at the metal-semiconductor contact region by acting as an electron trap to facilitate the charge separation of the hole-electron pair. It also promotes the interfacial electron transfer process, thereby increasing the photocatalytic activity of TiO_2.[19] However, a high silver content may be detrimental due the TiO_2 surface may become be covered by the Ag nanoparticles and the absorption of photons be decreased, thereby decreasing its photocatalytic activity.

4. Conclusions

Several TiO_2 photocatalysts with different amounts of Ag nanoparticles were prepared in aqueous medium without the presence of sacrificial agents. The effect of the photodeposition of the Ag nanoparticles on TiO_2 was evaluated by several model reactions such as the photodegradation of methyl orange dye, the photoproduction of the superoxide ion and disinfection tests under UV-A irradiation conditions. According to microscopic observations, the cells were divided into fragments and their intracellular components were released during the

photocatalytic process. The silver nanoparticles acts as no recombination centers since the negatively charged silver sites can attract positively charged holes, providing a high efficiency of charge separation of the hole-electron pair.

Acknowledgements

This research has been supported by the project "*Development of Multifunctional Nanomaterials and Processing Technology for Eco-friendly Applications*" from The National Research Foundation of Korea. We also thank the National Institute for Nanotechnology, located at CIMAV-Chihuahua, Mexico for the TEM characterization.

Notes and references

[a] Department of Environmental Engineering, Sun Moon University, Galsan-Ri, Tangjung-Myon, Asan Chungnam 336-708, South Korea.

[b] Facultad de Ciencias Físico Matemáticas, Universidad Autónoma de Nuevo León, Av. Universidad S/N, San Nicolás de los Garza, 66450 Nuevo León, México.

[c] Instituto de Ciencia de Materiales de Sevilla, Centro Mixto Universidad de Sevilla-CSIC. C/Américo Vespucio, 49, 41092 Sevilla, Spain. E-mail: sergio.obregon@icmse.csic.es Tel: +34 954489536 ext. 909225

[d] División de Materiales Avanzados, IPICYT (Instituto Potosino de Investigación Científica y Tecnológica), Camino a la Presa San José 2055 Col. Lomas 4a. sección C.P. 78216, San Luis Potosí, S.L.P., México
E-mail: vicente.rdz@ipicyt.edu.mx Tel: +52 44483 42000 ext. 7295

1 B.A. Markert, A.M. Breure, H.G. Zechmeister, Trace Metals and other Contaminants in the Environment 6: Bioindicators and biomonitors, Elsevier, 2003.

2. S. K. Agarwal, Environmental Monitoring, APH Publishing, India, 2005.

3. G. Honsell, M.D. Bortoli, S. Boscolo, C. Dell'Aversano, C. Battocchi, G. Fontanive, A. Penna, F. Berti, S. Sosa, T. Yasumoto, P. Ciminiello, M. Poli, A. Tubaro, *Environ. Sci. Technol.* 2011, **45**, 7051.

4. N. McQuaid, A. Zamyadi, M. Prévost, D.F. Bird, S. Dorner, *J. Environ. Monit.* 2011, **13**, 455.

5. R. Dai, H. Liu, J. Qu, J. Ru, Y. Hou, *J. Hazard. Mat.* 2008, **153**, 470.

6. T. Matsunaga, R. Tomoda, T. Nakajima, H. Wake, *FEMS Microbial. Lett.* 1985, **29**, 211.

7. K. Gupta, R.P. Singh, A. Pandey, A. Pandey, *Beilstein J. Nanotechnol.* 2013, **4**, 345.

8. S. Khan, I.A. Qazi, I. Hashmi, M.A. Awan, N.S. Zaidi, *J Nanomater.* 2013, 2013, Article ID 531010.

9. C.A. Linkous, G.J. Carter, D.B. Locuson, A.J. Ouellette, D.K. Slattery, L.A. Smitha, *Environ. Sci. Technol.* 2000, **34**, 4754.

10. V. Rodríguez-González, S.O. Alfaro, L.M. Torres-Martínez, S.H. Cho, S.W. Lee, *Appl. Catal. B: Environ.* 2010, **98**, 229.

11. S.O. Alfaro, A. Martínez-de la Cruz, L.M. Torres-Martínez, S.W. Lee, *Catal. Commun.* 2010, **11**, 326.

12. S.W. Lee, S. Obregón-Alfaro, V. Rodríguez-González, *J. Photoch. Photobio. A* 2011, **221**, 71.

13. V. Rodríguez-González, S. Obregón-Alfaro, L.M. Lozano-Sánchez, Soo-Wohn Lee, *J. Mol. Catal. A: Chem.* 2012, **353-354**, 163.

14. X. Xu, X. Duan, Z. Yi, Z. Zhou, X. Fan, Y. Wang, *Catal. Commun.* 2010, **12**, 169.

15. S. Obregón Alfaro, V. Rodríguez-González, A.A. Zaldívar-Cadena, S.W. Lee, *Catal. Today* 2011, **166**, 166.

16. S. Saha, J.M. Wang, A. Pal, *Sep. Purif. Technol.* 2012, **89**, 147.

17. X.G. Hou, M.D. Huang, X.L. Wu, A.D. Liu, *Chem. Eng. J.* 2009, **146**, 42.

18. T. Ohno, K. Sarukawa, K. Tokieda, M. Matsumura, *J. Catal.* 2001, **203**, 82.

19. L. Kvítek, A. Panáek, J. Soukupová, M. Kolář, R. Veceřová, R. Prucek, M. Holecová, Zbořil. Radek, *J. Phys. Chem. C* 2008, **112**, 5825.

20. A. Sclafani, J.M. Herrmann, *J. Photoch. Photobio. A* 1998, **113**, 181.

21. Ch. Girginov, P. Stefchev, P. Vitanov, Hr. Dikov, *J. Eng. Sci. Tech. Rev.* 2011, **5**, 14.

22. A. Henglein, *J. Phys. Chem.* 1979, **83**, 2209.